4094

Calibration-free Multidimensional Universal Refocusing Pulse Design for 3D Reduced Field-of-View Prostate Imaging

Jiayao Yang[1], Jesus Ernesto Fajardo[2], Jeffrey A. Fessler[1,2,3], Vikas Gulani[2], Jon-Fredrik Nielsen[1,2,3], and Yun Jiang[2,3]
[1]Department of Electrical Engineering and Computer Science, University of Michigan, Ann Arbor, MI, United States, [2]Department of Radiology, University of Michigan, Ann Arbor, MI, United States, [3]Department of Biomedical Engineering, University of Michigan, Ann Arbor, MI, United States

Synopsis

Keywords: RF Pulse Design & Fields, RF Pulse Design & Fields, Reduced FOV; 3D EPI;

Motivation: Universal pulses have been shown to be robust to $B1^+$ inhomogeneity for brain imaging at 7T, without time-consuming online design. A similar approach may be useful for designing multidimensional RF pulses for the 3D prostate imaging at 3T.

Goal(s): To design a universal multidimensional refocusing pulse and demonstrate its potential use for reduced field-of-view imaging in the prostate.

Approach: A three-dimensional universal refocusing pulse was designed using 6 subjects and validated in 12 subjects and in vivo prostate imaging at 3T.

Results: The proposed 3D universal refocusing pulse achieved similar performance on seen and unseen subjects. We successfully acquired reduced field-of-view prostate images.

Impact: Our simulation and in vivo results demonstrated the potential to design one universal 3D refocusing pulses for most subjects in prostate imaging.

Introduction

The goal of this study is to design calibration-free multidimensional radiofrequency (RF) pulses using the concept of universal pulses [1] for reduced field-of-view (rFOV) prostate imaging. The use of multidimensional RF pulses in rFOV imaging could shorten the scan time or improve the spatial resolution. Previously, multidimensional RF pulses have been designed using an auto-differentiation method and spin-domain based optimization [2,3]. However, the performance of multidimensional pulses can be affected by B_0 and B_1^+ inhomogeneities, thus requiring a tailored design using individually measured B_0 and B_1^+ for each subject [4,5]. These tailored approaches are time-consuming, which prevents the further adoption of rFOV imaging in a clinical setting. The universal pulse concept has shown its robustness to B_1^+ inhomogeneities for parallel transmission at 7T. Similar to the brain imaging at 7T, prostate imaging at 3T is also strongly affected by the inhomogeneous B_0 and B_1^+. In this work, we designed three-dimensional (3D) spatially selective refocusing pulses by combining the universal pulse concept with our spin-domain RF optimization [2]. We validated the performance of newly designed 3D RF pulses in numerical simulations and in vivo prostate imaging at 3T.

Methods

RF pulse design: The 3D spatially selective universal pulse design problem in the spin-domain was formulated as the following optimization problem

$$\arg\min_{\boldsymbol{b},\boldsymbol{g}} \mathrm{L} = \sum_{\mathrm{s}=1}^{\mathrm{S}} \left(\sum_{\mathrm{i}=1}^{\mathrm{M}} \mathrm{w_i} |\beta_{\mathrm{i}}^2(\boldsymbol{b},\boldsymbol{g};\mathrm{s}) - \beta_{\mathrm{D,i}}^2| \right)^{\mathrm{p}}, \quad \text{subject to} \quad \text{hardware limits},$$

where $\boldsymbol{b}$ is the RF waveform, $\boldsymbol{g}$ is gradient waveforms, β_{i}^2 and $\beta_{\mathrm{D,i}}^2 = -1$ are simulated and desired spin-domain parameters representing the refocusing efficiency, $\mathrm{w_i}$ is the weight for each spin, M is the total number of spins, and S is the total number of subjects used. Instead of directly minimizing the maximum error for each subject [1], we used p-norm ($\mathrm{p} = 4$) to approximate the infinity norm and performed the minimization by alternatingly updating $\boldsymbol{b}$ and $\boldsymbol{g}$. We constrained the optimization within the hardware limitations (i.e., peak B_1 of 0.25 mT, the maximum gradient amplitude of 50 mT/m and the maximum slew rate of 120 mT/m/ms).
We implemented this optimization in PyTorch using auto-differentiation with B_0 and B_1^+ measured from the pelvic region of 6 subjects. A refocusing pulse for a target region-of-interest (ROI) of $10 \times 10 \times 6\mathrm{cm}^3$ with a matrix size of $40 \times 40 \times 25$ was designed to cover the prostate gland. The design was initialized by the small-tip-angle approximation [6].
Numerical Simulations: Together with the universal pulse, RF pulses without considering B_0 and B_1^+ and tailored for specific B_0 and B_1^+ were also designed. The performance of these RF pulses was evaluated in simulations using B_0 and B_1^+ acquired from additional 12 subjects at 3T.
In vivo validation: The 3D spatially selective universal pulse was inserted into a 3D spin-echo stack-of-EPIs sequence by replacing the conventional refocusing pulse using Pulseq [7]. The method covered an FOV of $152 \times 152 \times 96\mathrm{mm}^3$ with a matrix size of $152 \times 152 \times 32$ in 60 seconds. 7 subjects were scanned on a 3T scanner (Magnetom Vida, Siemens) to validate the performance of our designed RF pulse.

Results

Figure 1a shows prostate B_1^+ of 10 subjects measured at 3T. Figure 1b shows the correlation of B_1^+ among these subjects, with coefficients ranging from 0.65 to 1. It demonstrates that B_1^+ values of the pelvic region at 3T exhibit a high level of correlation, suggesting that a group of subjects may potentially be used to represent others.
Figure 2 shows the gradient waveform, its slew rate and k-space trajectory, and the optimized RF waveforms. The universal pulse was optimized over 12 hours using 6 subjects, the pulse designed without B_0 and B_1^+ and the tailored pulse were optimized over 2 hours.
Figure 3 shows the comparison of different RF pulses in simulations. Compared to the RF pulse designed without B_0 and B_1^+, the universal pulse achieves better performance in term of the refocusing efficiency in both seen and unseen subjects.
Figure 4 shows representative images from four subjects acquired using 3D EPI with the universal pulse, as well as corresponding T2 reference images. Our results demonstrate our designed universal pulse is effective in achieving rFOV refocusing for prostate imaging at 3T.

Conclusions and Discussion

In this study, we developed an algorithm that designs a multidimensional spatially selective universal refocusing pulse. We evaluated the performance of the RF pulse through simulations and in vivo prostate imaging. Our results show that a 3D universal pulse designed using 6 subjects could achieve similar performance on unseen subjects, indicating the potential to move the pulse design offline. Furthermore, our in vivo results validated that rFOV prostate imaging could be achieved for most subjects using universal pulses, which could lead to the possibility for achieving high-resolution diffusion imaging with 3D rFOV EPI imaging.

Acknowledgements

This study was supported by NIH grants R37CA263583 and R01CA208236, and Siemens Healthcare.

References

[1] Gras, Vincent, et al. "Universal pulses: a new concept for calibration-free parallel transmission." Magnetic resonance in medicine 77.2 (2017): 635-643.

[2] Luo, Tianrui, et al. "Joint Design of RF and gradient waveforms via auto-differentiation for 3D tailored excitation in MRI." IEEE Transactions on Medical Imaging 40.12 (2021): 3305-3314.

[3] Yang, Jiayao, et al. "Multidimensional RF pulse design in spin-domain using auto-differentiation for 3D refocusing pulse", 2023 ISMRM Annual Meeting, Toronto, ON, Canada

[4] Hao, Sun, et al. "Joint design of excitation k-space trajectory and RF pulse for small-tip 3D tailored excitation in MRI." IEEE transactions on medical imaging 35.2 (2015): 468-479.

[5] Setsompop, Kawin, et al. "Magnitude least squares optimization for parallel radio frequency excitation design demonstrated at 7 Tesla with eight channels." Magnetic Resonance in Medicine: An Official Journal of the International Society for Magnetic Resonance in Medicine 59.4 (2008): 908-915.

[6] Pauly, John, et al. "A k-space analysis of small-tip-angle excitation." Journal of Magnetic Resonance (1969)81.1 (1989): 43-56.

[7] Layton, Kelvin J., et al. "Pulseq: a rapid and hardware-independent pulse sequence prototyping framework." Magnetic resonance in medicine 77.4 (2017): 1544-1552.

Figures

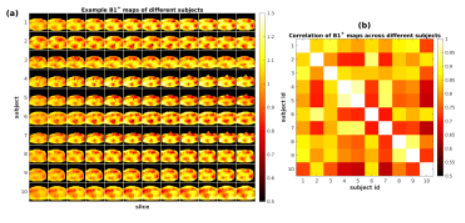

Figure 1. (a) B_1^+ maps acquired from 10 subjects. Each row contains 12 B_1^+ map slices from one subject. (b) Correlations between subjects. The correlation coefficient is between 0.65 and 1 which means the B_1^+ maps across the subjects have similarities.

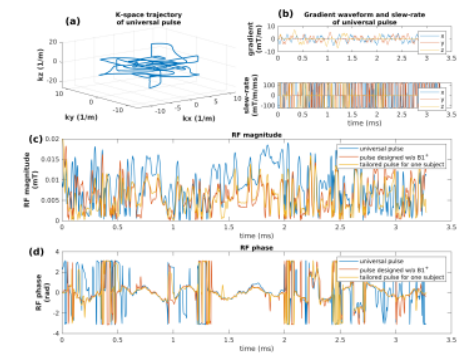

Figure 2. (a) Excitation k-space trajectory of the universal pulse, and (b) its corresponding gradient and the slew rate waveforms. (c) Magnitude of three optimized RF pulses. (d) Phase of three optimized pulses. The universal pulse was optimized using 6 subjects and the tailored pulse in the above plot was optimized specifically for each subject's B_0 and B_1^+ maps. (c)(d) also indicate that the design using several subjects leads to different solutions than the tailored design.

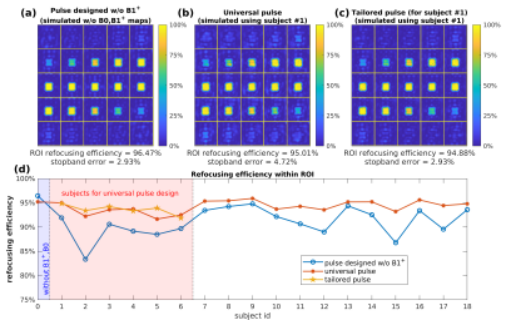

Figure 3. (a)-(c) Simulated refocusing efficiency for three different pulses. The 3D profiles are consistent with desired region-of-interest (ROI). (d) Simulated refocusing efficiency across different subjects, where the subjects 1-6 were used for universal pulse design and subjects 7-18 were not used. We also designed the tailored pulses for subjects 1-6 to represent the best performance we could achieve for each subject. For the simulated average error of region outside of the ROI of three RF pulses are all between 2% and 5 % for all subjects.

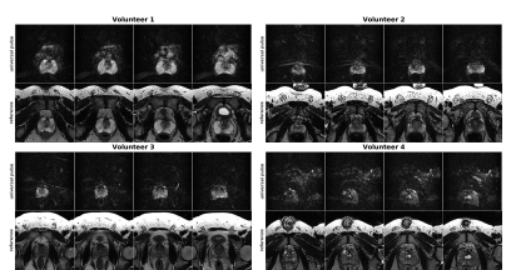

Figure 4. Four examples of 3D reduced FOV prostate images (four slices contains the prostate were shown) and their reference T2-weighted images (were cropped to the similar FOV size) from clinical protocol at 3T. The 3D rFOV images (FOV=152 × 152 × 96 mm^3) were acquired with universal pulse using spin-echo with stack-of-EPI acquisition using 60 seconds (TE=120ms, TR=1.8s, acquisition matrix size=152 × 152 × 32), and 75% partial Fourier was used in the acquisition.

Proc. Intl. Soc. Mag. Reson. Med. 32 (2024)
4094